Wavelet Adaptive Backstepping Control for a Class of Nonlinear Systems

Chun-Fei Hsu, *Member, IEEE*, Chih-Min Lin, *Senior Member, IEEE*, and Tsu-Tian Lee, *Fellow, IEEE*

***Abstract*—This paper proposes a wavelet adaptive backstepping control (WABC) system for a class of second-order nonlinear systems. The WABC comprises a neural backstepping controller and a robust controller. The neural backstepping controller containing a wavelet neural network (WNN) identifier is the principal controller, and the robust controller is designed to achieve L_2 tracking performance with desired attenuation level. Since the WNN uses wavelet functions, its learning capability is superior to the conventional neural network for system identification. Moreover, the adaptation laws of the control system are derived in the sense of Lyapunov function and Barbalat's lemma, thus the system can be guaranteed to be asymptotically stable. The proposed WABC is applied to two nonlinear systems, a chaotic system and a wing-rock motion system to illustrate its effectiveness. Simulation results verify that the proposed WABC can achieve favorable tracking performance by incorporating of WNN identification, adaptive backstepping control, and L_2 robust control techniques.**

***Index Terms*—Adaptive control, backstepping control, chaotic system, robust control, wavelet neural network (WNN), wing-rock system.**

I. Introduction

RECENTLY, the neural network-based control technique has represented an alternative method to solve control problems [1]–[6]. The most useful property of neural networks is their ability to approximate arbitrary linear or nonlinear mapping through learning. Based on their approximation ability, the neural networks have been used for approximation of control system dynamics or controllers. The basic issues in neural network feedback control are to provide online learning algorithms that do not require preliminary offline tuning. Some of these online learning algorithms are based on the backpropagation learning algorithm [2], and some are based on the Lyapunov stability theorem [1], [3]–[6]. Recently, some researchers have developed the structure of neural network based on the wavelet functions to construct the wavelet neural network (WNN) [7]–[10]. Unlike the sigmoidal functions used in conventional neural networks, wavelet functions are spatially localized, so that the learning capability of WNN is more efficient than the conventional sigmoidal function neural network for system identification. The training algorithms for WNN typically converge in a smaller number of iterations than for the conventional neural networks [7]. There has been considerable interest in exploring the applications of WNN to deal with nonlinearity and uncertainties of real-time servo control system [11]–[14]. These WNN controllers combine the capability of artificial neural networks for learning ability and the capability of wavelet decomposition for identification ability. Thus, the WNN-based control systems can achieve better control performance than NN-based control systems.

In the past decade, backstepping design procedures have been intensively introduced [15]–[18]. The backstepping control is a systematic and recursive design methodology for nonlinear systems to offer a choice to accommodate the unmodeled nonlinear effects and parameter uncertainties. The essence of backstepping design is to select recursively some appropriate functions of state variables as pseudocontrol inputs for lower dimension subsystems of the overall system. Each backstepping stage results in a new pseudocontrol design, expressed in terms of the pseudocontrol designs from preceding design stages. When the procedure is terminated, a feedback design for the true control input results, which achieves the original design objective by virtue of a final Lyapunov function, which is formed by summing up the Lyapunov functions associated with each individual design stage [15].

Robust control techniques have been used as the system is subject to bounded external disturbances whose upper bound is unknown. Combing the robust control with adaptive fuzzy control, some robust adaptive fuzzy control approaches have been proposed to attenuate the effects of approximation error to a prescribed level [19]–[21].

This paper proposes a wavelet adaptive backstepping control (WABC) system for a class of second-order nonlinear systems; this control system combines the advantages of WNN identification, adaptive backstepping control, and L_2 robust control techniques. The proposed WABC is comprised of a neural backstepping controller and a robust controller. The neural backstepping controller containing a WNN identifier is designed in the sense of the backstepping control technique, and the WNN identifier is utilized to online estimate the system dynamic function. The robust controller is designed to achieve L_2 tracking performance by attenuating the effect of the approximation error caused by the WNN identifier. The adaptive laws of the WABC system are derived in the sense of Lyapunov function and Barbalat's lemma; thus the system can be guaranteed to be asymptotically stable. Finally, a chaotic system and a wing-rock motion system are provided as the simulation examples to verify

Manuscript received June 28, 2004; revised February 14, 2005. This work was supported in part by the National Science Council of Republic of China under Grant NSC 92-2213-E-009-009.

C.-F. Hsu is with the Department of Electrical and Control Engineering, National Chiao-Tung University, Hsinchu 300, Taiwan, R.O.C. (e-mail: fei@cn.nctu.edu.tw).

C.-M. Lin is with the Department of Electrical Engineering, Yuan-Ze University, Chung-Li 320, Taiwan, R.O.C. (e-mail: cml@saturn.yzu.edu.tw).

T.-T. Lee is with the Department of Electrical Engineering, National Taipei University of Technology, Taipei 106, Taiwan, R.O.C. (e-mail: ttlee@ntut.edu.tw).

Digital Object Identifier 10.1109/TNN.2006.878122

that the proposed WABC scheme can achieve favorable tracking performance with regard to parameter variations and unknown dynamic function.

II. Design of Ideal Backstepping Controller

Consider a class of second-order nonlinear systems

$$\ddot{x} = f(x, \dot{x}) + u \tag{1}$$

where x is the state trajectory of the system, which is assumed to be available for measurement, $f(x, \dot{x})$ is a unknown real continuous function, and u is the input of the system. The control objective is to find a control law so that the state trajectory x can track a trajectory command x_c closely. Assuming that the parameters of the system (1) are known, the design of ideal backstepping controller is described step-by-step as follows.

Step 1) Define the tracking error

$$e_1 = x - x_c \tag{2}$$

and the derivative of tracking error is defined as

$$\dot{e}_1 = \dot{x} - \dot{x}_c. \tag{3}$$

The $\dot{x}$ can be viewed as a virtual control in the equation. Define the following stabilizing function

$$\delta = -c_1 e_1 + \dot{x}_c \tag{4}$$

where c_1 is a positive constant.

Step 2) Define

$$e_2 = \dot{x} - \delta \tag{5}$$

then the derivative of e_2 is expressed as

$$\dot{e}_2 = \ddot{x} - \dot{\delta} = \ddot{x} - (-c_1\dot{e}_1 + \ddot{x}_c) = \ddot{e}_1 + c_1\dot{e}_1. \tag{6}$$

Step 3) If the system dynamic function is known, the ideal backstepping controller can be obtained as

$$u_{ib} = \ddot{x}_c - f(x, \dot{x}) - c_1\dot{e}_1 - c_2 e_2 - e_1 \tag{7}$$

where c_2 is a positive constant. Substitution of (7) into (1) yields

$$\dot{e}_2 = -c_2 e_2 - e_1. \tag{8}$$

Step 4) Define a Lyapunov function as

$$V_1 = \frac{e_1^2}{2} + \frac{e_2^2}{2}. \tag{9}$$

Differentiating (9) with respect to time and using (3), (6), and (8), it is obtained that

$$\begin{aligned} \dot{V}_1 &= e_1\dot{e}_1 + e_2\dot{e}_2 \\ &= e_1(e_2 - c_1 e_1) + e_2(-c_2 e_2 - e_1) \\ &= -c_1 e_1^2 - c_2 e_2^2 \le 0. \end{aligned} \tag{10}$$

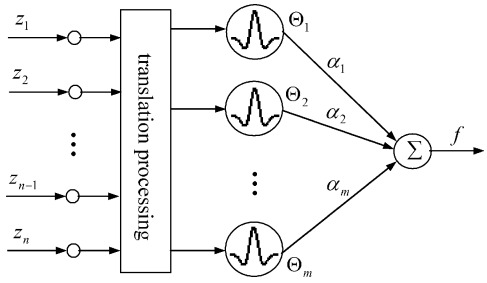

Fig. 1. Network structure of a WNN.

Since $\dot{V}_1 \le 0$, that is $V_1(t) \le V_1(0)$, it implies that e_1 and e_2 are bounded. Now define the following term:

$$\Omega = c_1 e_1^2 + c_2 e_2^2 = -\dot{V}_1 \tag{11}$$

then

$$\int_0^t \Omega(\tau) d\tau = V_1(0) - V_1(t). \tag{12}$$

Because $V_1(0)$ is bounded and $V_1(t)$ is nonincreasing and bounded, the following result can be obtained:

$$\lim_{t\to\infty} \int_0^t \Omega(\tau)\, d\tau < \infty. \tag{13}$$

Also $\dot{\Omega}$ is bounded, so by Barbalat's Lemma [22], it can be shown that $\lim_{t\to\infty} \Omega = 0$. This implies that e_1 and e_2 converge to zero as $t \to \infty$. Therefore, the ideal backstepping controller in (7) will asymptotically stabilize the system.

III. Design of Wavelet Adaptive Backstepping Controller

Since the system dynamic function $f(x, \dot{x})$ may be unknown or perturbed in practical application, the ideal backstepping controller (7) cannot be precisely obtained. To solve this problem, a WNN identifier is utilized to approximate the system dynamic function. The descriptions of the WNN identifier and the design steps of the control system are described as follows.

A. WNN Identifier

The network structure of the WNN identifier is shown in Fig. 1, which can be considered as "1"-layer feedforward neural network with input preprocessing element. The WNN output with m wavelet basis functions can perform the mapping according to [7]

$$f(\mathbf{z}) = \sum_{j=1}^{m} \alpha_j \Theta_j(\boldsymbol{\omega}_j, (\mathbf{z} - \mathbf{c}_j)) \tag{14}$$

where $\mathbf{z} = [z_1\, z_2 \ldots z_n]^T \in R^n$ is the input vector, $\Theta_j(\boldsymbol{\omega}_j, (\mathbf{z} - \mathbf{c}_j)) \in R$, $j = 1, 2, \ldots, m$ are the wavelet

functions, $\boldsymbol{\omega}_j = [\omega_{1j}\,\omega_{2j}\,\ldots\,\omega_{nj}]^T \in R^n$ and $\mathbf{c}_j = [c_{1j}\,c_{2j}\,\ldots\,c_{nj}]^T \in R^n$ are the dilation and translation parameters, respectively, $\alpha_j \in R$ is the output layer weight, and m is the number of units (also called nodes and neurons) in the translation layer. Each wavelet network's neuron in the translation layer can be represented by

$$\Theta_j = h_j(\mathbf{z}) \exp\left(-\frac{\sum_{k=1}^{n} \omega_{kj}^2 (z_k - c_{kj})^2}{2} \right) \tag{15}$$

where the "Mexican hat" mother wavelet function is defined as $h_j(\mathbf{z}) = \prod_{k=1}^{n} (1 - w_k^2 z_k^2)$. For ease of notation, (14) can be expressed in a compact vector form as

$$f(\mathbf{z}, \boldsymbol{\alpha}, \boldsymbol{\omega}, \mathbf{c}) = \boldsymbol{\alpha}^T \boldsymbol{\Theta}(\mathbf{z}, \boldsymbol{\omega}, \mathbf{c}) \tag{16}$$

where $\boldsymbol{\alpha} = [\alpha_1\,\alpha_2\,\ldots\,\alpha_m]^T \in R^m$, $\boldsymbol{\Theta} = [\Theta_1\,\Theta_2\,\ldots\,\Theta_m]^T \in R^m$, $\boldsymbol{\omega} = [\boldsymbol{\omega}_1\,\boldsymbol{\omega}_2\,\ldots\,\boldsymbol{\omega}_m]^T \in R^{n\times m}$, and $\mathbf{c} = [\mathbf{c}_1\,\mathbf{c}_2\,\ldots\,\mathbf{c}_m]^T \in R^{n\times m}$. By the universal approximation theorem, there exists an ideal WNN identifier f^* such that [7]

$$f = f^*(\mathbf{z}) + \Delta = \boldsymbol{\alpha}^{*T} \boldsymbol{\Theta}(\mathbf{z}, \boldsymbol{\omega}^*, \mathbf{c}^*) + \Delta \tag{17}$$

where Δ denotes the approximation error and is assumed to be bounded by $|\Delta| \le \Delta^*$, in which Δ^* is a positive constant; and $\boldsymbol{\omega}^*$, $\mathbf{c}^*$, and $\boldsymbol{\alpha}^*$ are the optimal parameter vectors of $\boldsymbol{\omega}$, $\mathbf{c}$, and $\boldsymbol{\alpha}$, respectively. In fact, the optimal parameter vectors that are needed to best approximate a given nonlinear function are difficult to determine. Thus, an estimate function is defined as

$$\hat{f}(\mathbf{z}, \hat{\boldsymbol{\alpha}}, \hat{\boldsymbol{\omega}}, \hat{\mathbf{c}}) = \hat{\boldsymbol{\alpha}}^T \boldsymbol{\Theta}(\mathbf{z}, \hat{\boldsymbol{\omega}}, \hat{\mathbf{c}}) \tag{18}$$

where $\hat{\boldsymbol{\omega}}$, $\hat{\mathbf{c}}$, and $\hat{\boldsymbol{\alpha}}$ are the estimation of $\boldsymbol{\omega}^*$, $\mathbf{c}^*$, and $\boldsymbol{\alpha}^*$, respectively. For notational convenience, denote $\boldsymbol{\Theta}^* = \boldsymbol{\Theta}(\mathbf{z}, \boldsymbol{\omega}^*, \mathbf{c}^*)$ and $\hat{\boldsymbol{\Theta}} = \boldsymbol{\Theta}(\mathbf{z}, \hat{\boldsymbol{\omega}}, \hat{\mathbf{c}})$. Define the estimated error as

$$\tilde{f} = f - \hat{f} = f^* - \hat{f} + \Delta = \tilde{\boldsymbol{\alpha}}^T \tilde{\boldsymbol{\Theta}} + \hat{\boldsymbol{\alpha}}^T \tilde{\boldsymbol{\Theta}} + \tilde{\boldsymbol{\alpha}}^T \hat{\boldsymbol{\Theta}} + \Delta \tag{19}$$

where $\tilde{\boldsymbol{\alpha}} = \boldsymbol{\alpha}^* - \hat{\boldsymbol{\alpha}}$ and $\tilde{\boldsymbol{\Theta}} = \boldsymbol{\Theta}^* - \hat{\boldsymbol{\Theta}}$. In the following, some tuning laws will be derived to online tune the parameters of the WNN identifier to achieve favorable estimation of the system dynamic function. To achieve this goal, the Taylor expansion linearization technique is employed to transform the nonlinear function into a partially linear form [5], i.e.,

$$\tilde{\boldsymbol{\Theta}} = \begin{bmatrix} \tilde{\Theta}_1 \\ \tilde{\Theta}_2 \\ \vdots \\ \tilde{\Theta}_m \end{bmatrix} = \begin{bmatrix} \frac{\partial \Theta_1}{\partial \boldsymbol{\omega}} \\ \frac{\partial \Theta_2}{\partial \boldsymbol{\omega}} \\ \vdots \\ \frac{\partial \Theta_m}{\partial \boldsymbol{\omega}} \end{bmatrix} \Big|_{\boldsymbol{\omega}=\hat{\boldsymbol{\omega}}} \tilde{\boldsymbol{\omega}} + \begin{bmatrix} \frac{\partial \Theta_1}{\partial \mathbf{c}} \\ \frac{\partial \Theta_2}{\partial \mathbf{c}} \\ \vdots \\ \frac{\partial \Theta_m}{\partial \mathbf{c}} \end{bmatrix} \Big|_{\mathbf{c}=\hat{\mathbf{c}}} \tilde{\mathbf{c}} + \mathbf{h} \tag{20}$$

or

$$\tilde{\boldsymbol{\Theta}} = \mathbf{A}^T \tilde{\boldsymbol{\omega}} + \mathbf{B}^T \tilde{\mathbf{c}} + \mathbf{h} \tag{21}$$

where $\tilde{\boldsymbol{\omega}} = \boldsymbol{\omega}^* - \hat{\boldsymbol{\omega}}$; $\tilde{\mathbf{c}} = \mathbf{c}^* - \hat{\mathbf{c}}$; $\mathbf{h}$ is a vector of higher order terms; $\mathbf{A} = [(\partial\Theta_1/\partial\boldsymbol{\omega})(\partial\Theta_2/\partial\boldsymbol{\omega})\cdots(\partial\Theta_m/\partial\boldsymbol{\omega})]\,|_{\boldsymbol{\omega}=\hat{\boldsymbol{\omega}}}$; $\mathbf{B} = [(\partial\Theta_1/\partial\mathbf{c})(\partial\Theta_2/\partial\mathbf{c})\cdots(\partial\Theta_m/\partial\mathbf{c})]\,|_{\mathbf{c}=\hat{\mathbf{c}}}$; and $\partial\Theta_l/\partial\boldsymbol{\omega}$ and $\partial\Theta_l/\partial\mathbf{c}$ are defined as

$$\left[\frac{\partial \Theta_l}{\partial \boldsymbol{\omega}}\right]^T = \left[\underset{(l-1)\times n}{0\cdots 0} \frac{\partial \Theta_l}{\partial \omega_{1l}} \cdots \frac{\partial \Theta_l}{\partial \omega_{nl}} \underset{(m-l)\times n}{0\cdots 0}\right] \tag{22}$$

$$\left[\frac{\partial \Theta_l}{\partial \mathbf{c}}\right]^T = \left[\underset{(l-1)\times n}{0\cdots 0} \frac{\partial \Theta_l}{\partial c_{1l}} \cdots \frac{\partial \Theta_l}{\partial c_{nl}} \underset{(m-l)\times n}{0\cdots 0}\right]. \tag{23}$$

Substitution of (21) into (19) yields

$$\begin{aligned} \tilde{f} &= \tilde{\boldsymbol{\alpha}}^T (\mathbf{A}^T \tilde{\boldsymbol{\omega}} + \mathbf{B}^T \tilde{\mathbf{c}} + \mathbf{h}) + \hat{\boldsymbol{\alpha}}^T (\mathbf{A}^T \tilde{\boldsymbol{\omega}} + \mathbf{B}^T \tilde{\boldsymbol{c}} + \mathbf{h}) + \tilde{\boldsymbol{\alpha}}^T \hat{\boldsymbol{\Theta}} + \Delta \\ &= \tilde{\boldsymbol{\alpha}}^T \mathbf{A}^T (\boldsymbol{\omega}^* - \hat{\boldsymbol{\omega}}) + \tilde{\boldsymbol{\alpha}}^T \mathbf{B}^T (\mathbf{c}^* - \hat{\mathbf{c}}) + \tilde{\boldsymbol{\alpha}}^T \mathbf{h} \\ &\quad + \hat{\boldsymbol{\alpha}}^T \mathbf{A}^T \tilde{\boldsymbol{\omega}} + \hat{\boldsymbol{\alpha}}^T \mathbf{B}^T \tilde{\mathbf{c}} + \hat{\boldsymbol{\alpha}}^T \mathbf{h} + \tilde{\boldsymbol{\alpha}}^T \hat{\boldsymbol{\Theta}} + \Delta \\ &= \tilde{\boldsymbol{\alpha}}^T (\hat{\boldsymbol{\Theta}} - \mathbf{A}^T \hat{\boldsymbol{\omega}} - \mathbf{B}^T \hat{\mathbf{c}}) + \tilde{\boldsymbol{\omega}}^T \mathbf{A} \hat{\boldsymbol{\alpha}} + \tilde{\mathbf{c}}^T \mathbf{B} \hat{\boldsymbol{\alpha}} + \varepsilon \end{aligned} \tag{24}$$

where the uncertain term $\varepsilon = \tilde{\boldsymbol{\alpha}}^T \mathbf{A}^T \boldsymbol{\omega}^* + \tilde{\boldsymbol{\alpha}}^T \mathbf{B}^T \mathbf{c}^* + \boldsymbol{\alpha}^* \mathbf{h} + \Delta$.

B. WABC System

The proposed WABC system is shown in Fig. 2, which is comprised of a neural backstepping controller u_{nb} and a robust controller u_{ar}. The tracking error e_1 is defined in (2), a stabilizing function δ in (4), and e_2 in (5). The control law of the WABC is developed as follows:

$$u_{wc} = u_{nb} + u_{ar}. \tag{25}$$

The neural backstepping controller is chosen as

$$u_{nb} = \ddot{x}_c - \hat{f} - c_1 \dot{e}_1 - c_2 e_2 - e_1 \tag{26}$$

where the WNN identifier $\hat{f}$ is designed to online estimate the system dynamic function f. Substitution of (25) and (26) into (1) yields

$$\dot{e}_2 = f - \hat{f} - c_2 e_2 - e_1 + u_{ar}. \tag{27}$$

By substituting (24) into (27), we obtain

$$\begin{aligned} \dot{e}_2 = \tilde{\boldsymbol{\alpha}}^T (\hat{\boldsymbol{\Theta}} - \mathbf{A}^T \hat{\boldsymbol{\omega}} - \mathbf{B}^T \hat{\mathbf{c}}) + \tilde{\boldsymbol{\omega}}^T \mathbf{A} \hat{\boldsymbol{\alpha}} \\ + \tilde{\mathbf{c}}^T \mathbf{B} \hat{\boldsymbol{\alpha}} + \varepsilon - c_2 e_2 - e_1 + u_{ar}. \end{aligned} \tag{28}$$

Then, Theorem 1 shows the properties of the proposed WABC control system.

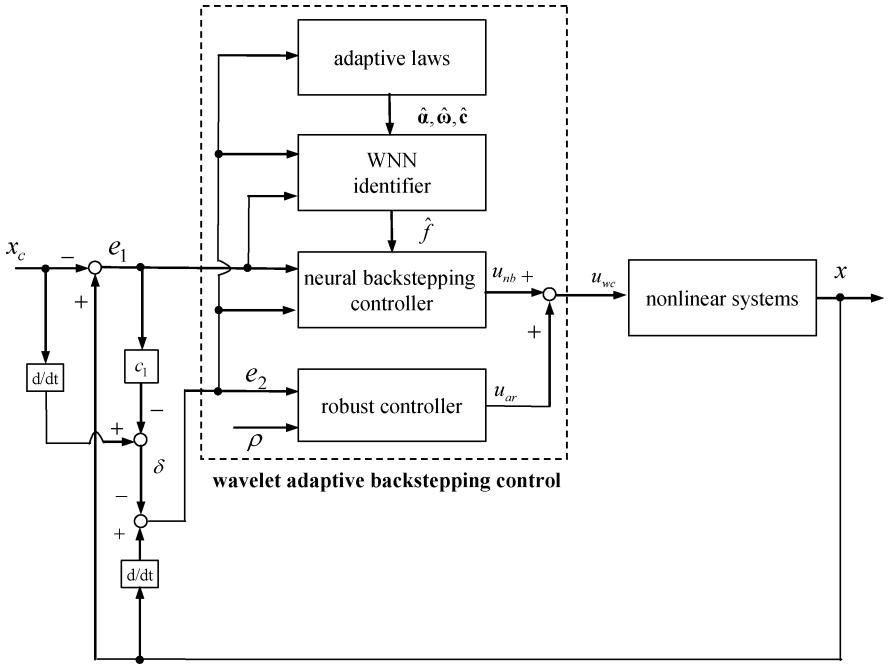

Fig. 2. WABC for nonlinear systems.

Theorem 1: Consider a nonlinear system represented by (1). The control system is designed as (25) where the neural backstepping controller is designed as (26), in which the adaptation laws of the WNN identifier are designed as

$$\dot{\hat{\boldsymbol{\alpha}}} = -\dot{\tilde{\boldsymbol{\alpha}}} = \eta_1 e_2(\hat{\boldsymbol{\Theta}} - \mathbf{A}^T\hat{\boldsymbol{\omega}} - \mathbf{B}^T\hat{\mathbf{c}}) \tag{29}$$

$$\dot{\hat{\boldsymbol{\omega}}} = -\dot{\tilde{\boldsymbol{\omega}}} = \eta_2 e_2 \mathbf{A}\hat{\boldsymbol{\alpha}} \tag{30}$$

$$\dot{\hat{\mathbf{c}}} = -\dot{\tilde{\mathbf{c}}} = \eta_3 e_2 \mathbf{B}\hat{\boldsymbol{\alpha}} \tag{31}$$

where η_1, η_2, and η_3 are the learning rates with positive constants, and the robust controller is designed as

$$u_{ar} = -\frac{(\rho^2+1)e_2}{2\rho^2} \tag{32}$$

where ρ is a prescribed attenuation constant. Then, the overall control scheme guarantees the following properties:

1)

$$c_1\int_0^T e_1^2(\tau)d\tau \le \frac{e_1^2(0)}{2} + \frac{e_2^2(0)}{2} + \frac{\tilde{\boldsymbol{\alpha}}^T(0)\tilde{\boldsymbol{\alpha}}(0)}{2\eta_1} + \frac{\tilde{\boldsymbol{\omega}}^T(0)\tilde{\boldsymbol{\omega}}(0)}{2\eta_2} + \frac{\tilde{\mathbf{c}}^T(0)\tilde{\mathbf{c}}(0)}{2\eta_3} + \frac{\rho^2}{2}\int_0^T \varepsilon^2(\tau)d\tau \tag{33}$$

where $T \in [0,\infty]$.

2) If ε is squared integrable, that is $\int_0^\infty \varepsilon^2 d\tau < \infty$, then $\lim_{t\to\infty}|e_1| = 0$.

Proof: Define a Lyapunov function as

$$V_2 = \frac{e_1^2}{2} + \frac{e_2^2}{2} + \frac{\tilde{\boldsymbol{\alpha}}^T\tilde{\boldsymbol{\alpha}}}{2\eta_1} + \frac{\tilde{\boldsymbol{\omega}}^T\tilde{\boldsymbol{\omega}}}{2\eta_2} + \frac{\tilde{\mathbf{c}}^T\tilde{\mathbf{c}}}{2\eta_3}. \tag{34}$$

Differentiating (34) with respect to time and using (2) and (28)–(32)

$$\begin{aligned}
\dot{V}_2 &= e_1\dot{e}_1 + e_2\dot{e}_2 + \frac{\tilde{\boldsymbol{\alpha}}^T\dot{\tilde{\boldsymbol{\alpha}}}}{\eta_1} + \frac{\tilde{\boldsymbol{\omega}}^T\dot{\tilde{\boldsymbol{\omega}}}}{\eta_2} + \frac{\tilde{\mathbf{c}}^T\dot{\tilde{\mathbf{c}}}}{\eta_3} \\
&= e_1(e_2 - c_1e_1) + e_2(\tilde{\boldsymbol{\alpha}}^T(\hat{\boldsymbol{\Theta}} - \mathbf{A}^T\hat{\boldsymbol{\omega}} - \mathbf{B}^T\hat{\mathbf{c}}) + \tilde{\boldsymbol{\omega}}^T\mathbf{A}\hat{\boldsymbol{\alpha}} \\
&\quad + \tilde{\mathbf{c}}^T\mathbf{B}\hat{\boldsymbol{\alpha}} + \varepsilon - c_2e_2 - e_1 + u_{ar}) + \frac{\tilde{\boldsymbol{\alpha}}^T\dot{\tilde{\boldsymbol{\alpha}}}}{\eta_1} + \frac{\tilde{\boldsymbol{\omega}}^T\dot{\tilde{\boldsymbol{\omega}}}}{\eta_2} + \frac{\tilde{\mathbf{c}}^T\dot{\tilde{\mathbf{c}}}}{\eta_3} \\
&= -c_1e_1^2 - c_2e_2^2 + \tilde{\boldsymbol{\alpha}}^T\left(e_2(\hat{\boldsymbol{\Theta}} - \mathbf{A}^T\hat{\boldsymbol{\omega}} - \mathbf{B}^T\hat{\mathbf{c}}) + \frac{\dot{\tilde{\boldsymbol{\alpha}}}}{\eta_1}\right) \\
&\quad + \tilde{\boldsymbol{\omega}}^T\left(e_2\mathbf{A}\hat{\boldsymbol{\alpha}} + \frac{\dot{\tilde{\boldsymbol{\omega}}}}{\eta_2}\right) + \tilde{\mathbf{c}}^T\left(e_2\mathbf{B}\hat{\boldsymbol{\alpha}} + \frac{\dot{\tilde{\mathbf{c}}}}{\eta_3}\right) + e_2(\varepsilon + u_{ar}) \\
&= -c_1e_1^2 - c_2e_2^2 + \varepsilon e_2 - \frac{(\rho^2+1)e_2^2}{2\rho^2} \\
&= -c_1e_1^2 - c_2e_2^2 - \frac{e_2^2}{2} - \frac{1}{2}\left(\frac{e_2}{\rho} - \rho\varepsilon\right)^2 + \frac{\rho^2\varepsilon^2}{2} \\
&\le -c_1e_1^2 + \frac{\rho^2\varepsilon^2}{2}.
\end{aligned} \tag{35}$$

Integrating (35) from $t = 0$ to $t = T$, yields

$$V_2(T) - V_2(0) \le -c_1\int_0^T e_1^2(\tau)d\tau + \frac{\rho^2}{2}\int_0^T \varepsilon^2(\tau)d\tau. \tag{36}$$

Since $V_2(T) \ge 0$, (36) implies the following:

$$c_1\int_0^T e_1^2(\tau)d\tau \le V_2(0) + \frac{\rho^2}{2}\int_0^T \varepsilon^2(\tau)d\tau. \tag{37}$$

Using (34), (37) is equivalent to (33). Since $V_2(0)$ is finite, if the approximation error $\varepsilon \in L_2$, that is $\int_0^T \varepsilon^2(\tau)d\tau < \infty$, using the Barbalat's lemma [22], it implies that $\lim_{t\to\infty}|e_1| = 0$.

Remark 1: The inequality (33) reveals that the integrated squared error of e_1 is less than or equal to the sum of some initial squared errors, some parameter initial squared value and the integrated squared error of ε. Since the initial squared errors and parameter initial squared value are finite, if ε is squared integrable then we can conclude that e_1 will approach to zero.

Remark 2: If the system starts with initial conditions $e_1(0) = 0$, $e_2(0) = 0$, $\tilde{\boldsymbol{\alpha}}(0) = 0$, $\tilde{\boldsymbol{\omega}}(0) = 0$, and $\tilde{\mathbf{c}}(0) = 0$, then the L_2 performance in (33) can be rewritten as

$$\sup_{\varepsilon \in L_2[0,T]} \frac{\int_0^T e_1^2(\tau)d\tau}{\int_0^T \varepsilon^2(\tau)d\tau} \leq \frac{\rho^2}{2c_1} \tag{38}$$

where the L_2-gain from ε to the e_1 must be equal to or less than a level $\rho^2/2c_1$ [19]–[21].

IV. Simulation Results

In this section, the proposed WABC technique is applied to control two nonlinear systems: a chaotic system (Example 1) and a wing-rock motion system (Example 2). It should be emphasized that development of the WABC does not require the knowledge of the system dynamic function.

1) Example 1 (Chaotic System): Chaotic systems have been known to exhibit complex dynamical behavior. Several control techniques have been proposed for the chaotic systems [23], ; however, some of them cannot achieve favorable control performance and some of them require system dynamic function. Consider a second-order chaotic system such as well known Duffing's equation describing a special nonlinear circuit or a pendulum moving in a viscous medium under control [23]

$$\ddot{x} = -p\dot{x} - p_1 x - p_2 x^3 + q\cos(wt) + u = f(x, \dot{x}) + u \tag{39}$$

where p, p_1, p_2, and q are real constants; t is the time variable; w is the frequency; $f(x, \dot{x}) = -p\dot{x} - p_1 x - p_2 x^3 + q\cos(wt)$ is the system dynamic function; and u is the control effort. Depending on the choice of these constants, it is known that the solutions of system (39) may exhibit periodic, almost periodic, and chaotic behavior. For observing the chaotic unpredictable behavior, the open-loop system behavior with $u = 0$ was simulated with $p = 0.4$, $p_1 = -1.1$, $p_2 = 1.0$, and $w = 1.8$. The phase plane plots from an initial condition point (1,1) are shown in Fig. 3(a)–(c) for $q = 0.62$, $q = 1.95$, and $q = 7.00$, respectively. It is shown that the uncontrolled chaotic system has different trajectories for different q values.

The system dynamic function would be online estimated by the WNN identifier. A WNN identifier with five hidden nodes is utilized to approach the system dynamic function of the chaotic system. In addition, the control parameters are selected as $c_1 = c_2 = 1$, $\eta_1 = \eta_2 = \eta_3 = 10$, and $w_k = 0.8$ for $k = 1, 2, \ldots, 5$. These parameters are chosen through some trials to achieve favorable transient control performance. The trajectory command is set as $x_c = \cos(t)$. The simulation results of the WABC for $q = 0.62$, $q = 1.95$, and $q = 7.00$ are shown in Figs. 4–6, respectively. For the attenuation level $\rho = 0.5$, the tracking responses of state x are shown in Figs. 4(a)–6(a); the tracking responses of state $\dot{x}$ are shown in Figs. 4(b)–6(b); and the associated control efforts are shown in Figs. 4(c)–6(c), respectively. Moreover, to achieve smaller attenuation level, the case

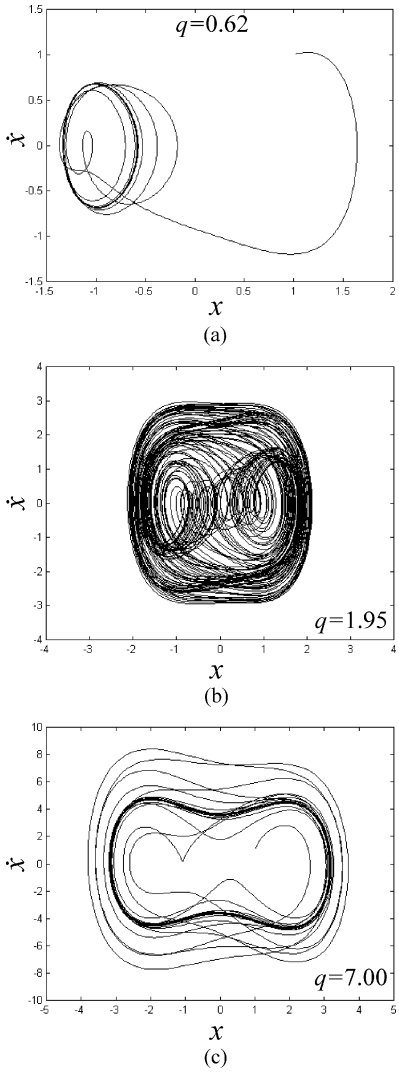

Fig. 3. Phase plane of uncontrolled chaotic system.

for $\rho = 0.2$ is reconsidered. In this case, the tracking responses of state x are shown in Figs. 4(d)–6(d); the tracking responses of state $\dot{x}$ are shown in Figs. 4(e)–6(e); and the associated control efforts are shown Figs. 4(f)–6(f), respectively. A performance index I is defined as $I = \sqrt{e_1^2 + \dot{e}_1^2}$. The performance index I is shown in Figs. 4(g)–6(g), respectively. It is shown that the proposed WABC can achieve favorable tracking performance; moreover, the better tracking performance can be achieved as specified attenuation level ρ is chosen smaller.

2) Example 2 (Wing-Rock Motion System): Some combat aircrafts often operate at subsonic speeds and high angles of attack. These aircrafts may become unstable due to oscillation, mainly a rolling motion known as wing-rock motion [24], [25]. A dynamic system of the wing-rock motion system can be written in a state variable form as

$$\begin{aligned}\ddot{x} &= b_0 + b_1 x + b_2 \dot{x} + b_3 |x| \dot{x} + b_4 |\dot{x}| \dot{x} + b_5 x^3 + u \\ &= f(x, \dot{x}) + u\end{aligned} \tag{40}$$

where x is the roll angle and the parameters b_i, $i = 0, 1, \ldots, 5$ are nonlinear functions of the angle of attack. The aerodynamic parameters are given by $b_0 = 0$, $b_1 = -0.01859521$, $b_2 =$

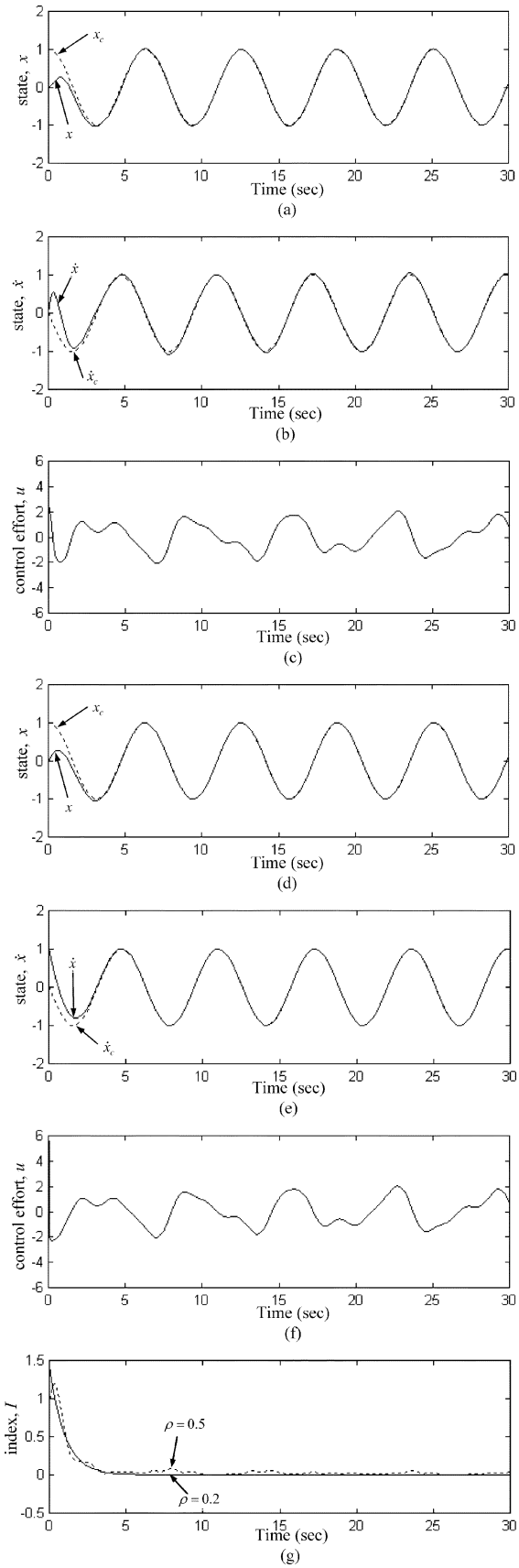

Fig. 4. Simulation results of chaotic system for $q = 0.62$.

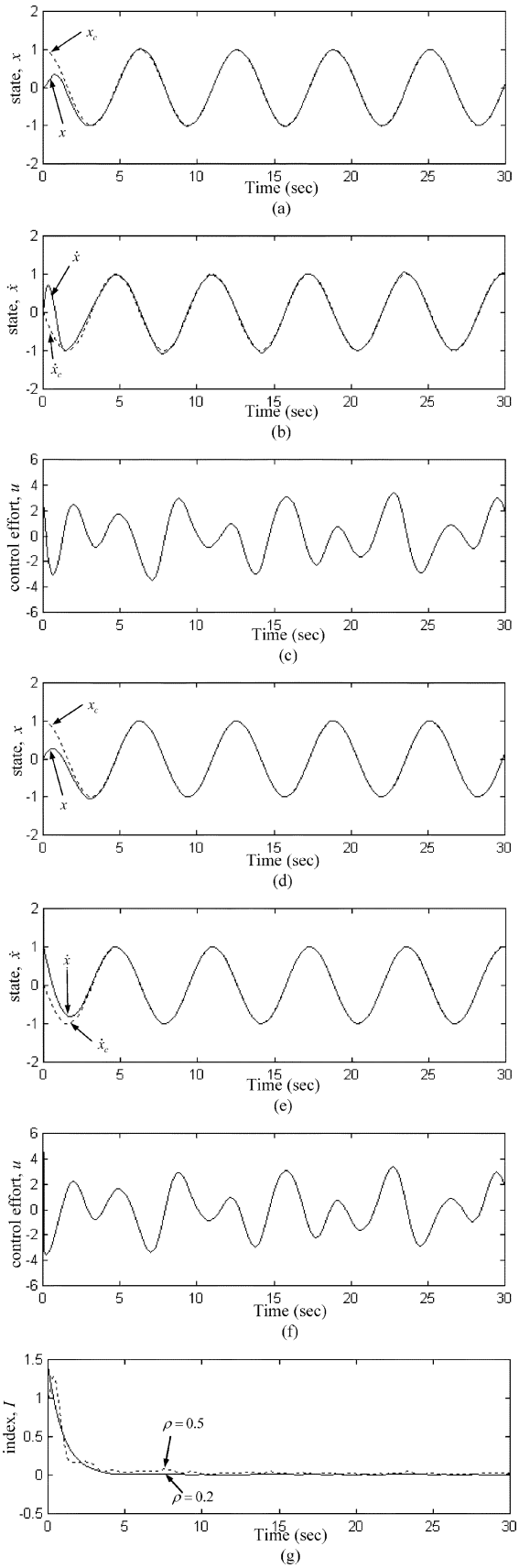

Fig. 5. Simulation results of chaotic system for $q = 1.95$.

0.015162375, $b_3 = -0.06245153$, $b_4 = 0.00954708$, and $b_5 = 0.02145291$. The open-loop system time response with $u = 0$ was simulated for two initial conditions: a small initial condition ($x = 6°$, $\dot{x} = 3° \cdot \mathrm{s}^{-1}$) and a large initial condition ($x = 30°$,

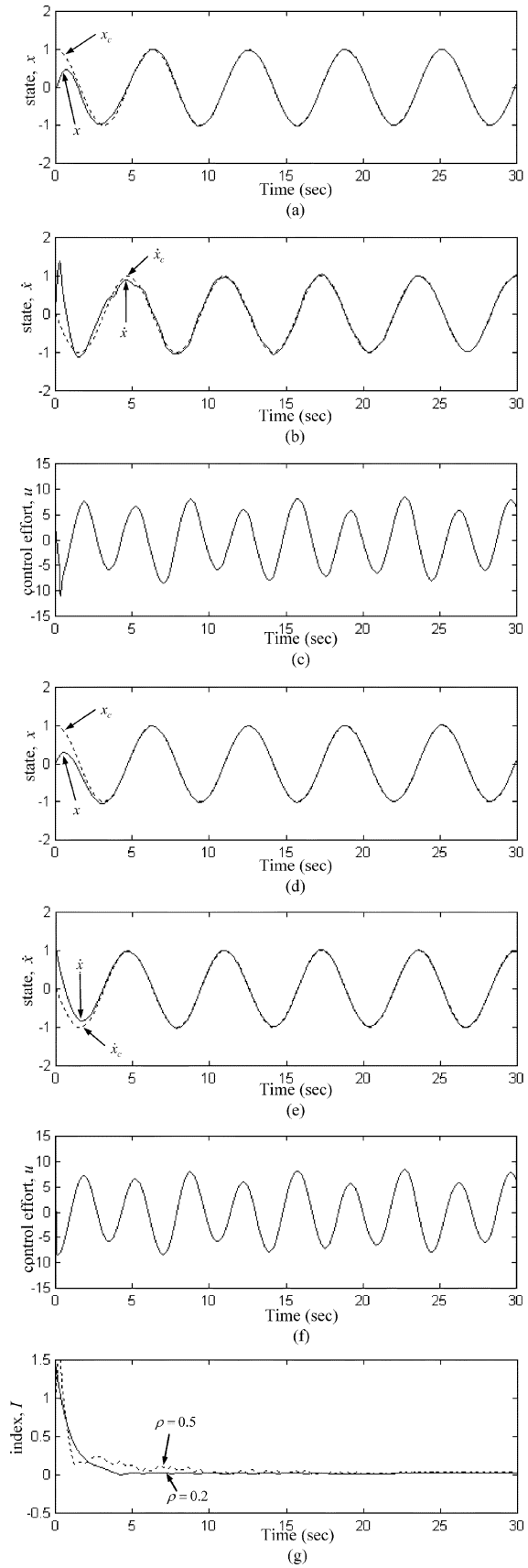

Fig. 6. Simulation results of chaotic system for $q = 7.00$.

$\dot{x} = 10^{\circ} \cdot \mathrm{s}^{-1}$). The phase-plane plot is shown in Fig. 7. For the small initial condition, a limit cycle oscillation is obtained, and

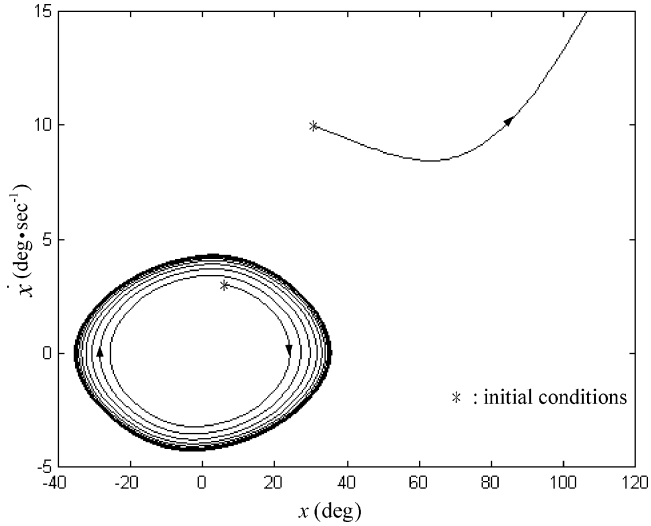

Fig. 7. Phase-plane portrait of uncontrolled wing-rock motion system.

for the large initial condition, the roll angle is divergent. Thus, it is shown that the uncontrolled nonlinear wing-rock motion system will be unstable for some initial conditions.

The system dynamic function would be online estimated by the WNN identifier. A WNN identifier with five hidden nodes is utilized to approach the system dynamic function of the wing-rock motion system. In addition, the control parameters are selected as $c_1 = c_2 = 0.5$, $\eta_1 = \eta_2 = \eta_3 = 20$, and $w_k = 0.7$ for $k = 1, 2, \ldots, 5$. These parameters are chosen through some trials to achieve favorable transient control performance. The simulation results of the WABC for small and large initial conditions are shown in Figs. 8 and 9, respectively. For the attenuation level $\rho = 0.5$, the tracking responses of state x are shown in Figs. 8(a) and 9(a); and the associated control efforts are shown Figs. 8(b) and 9(b), respectively. Moreover, to achieve smaller attenuation level, the case for $\rho = 0.2$ is reconsidered. In this case, the tracking responses of state x are shown in Figs. 8(c) and 9(c); and the associated control efforts are shown Figs. 8(d) and 9(d), respectively. A performance index I is defined as $I = \sqrt{e_1^2 + \dot{e}_1^2}$. The performance index I is shown in Figs. 8(e) and 9(e), respectively. It is shown that the proposed WABC can achieve favorable tracking performance. Similar to the chaotic system (Example 1), the better tracking performance can be achieved as specified attenuation level ρ is chosen smaller.

V. Conclusion

For some systems, since the dynamic characteristics of the control system are nonlinear and the precise models are difficult to obtain, the model-based control approaches are difficult to be implemented. To overcome this drawback, a novel WABC system has been proposed. The developed WABC system is comprised of a neural backstepping controller and a robust controller. In the neural backstepping controller, a WNN identifier is utilized to online estimate the system dynamic function. The adaptive laws of the WABC system are synthesized using the Lyapunov function and Barbalat's lemma so that the asymptotic stability of the control system can be guaranteed. The contributions of the proposed design method are the use of WNN to

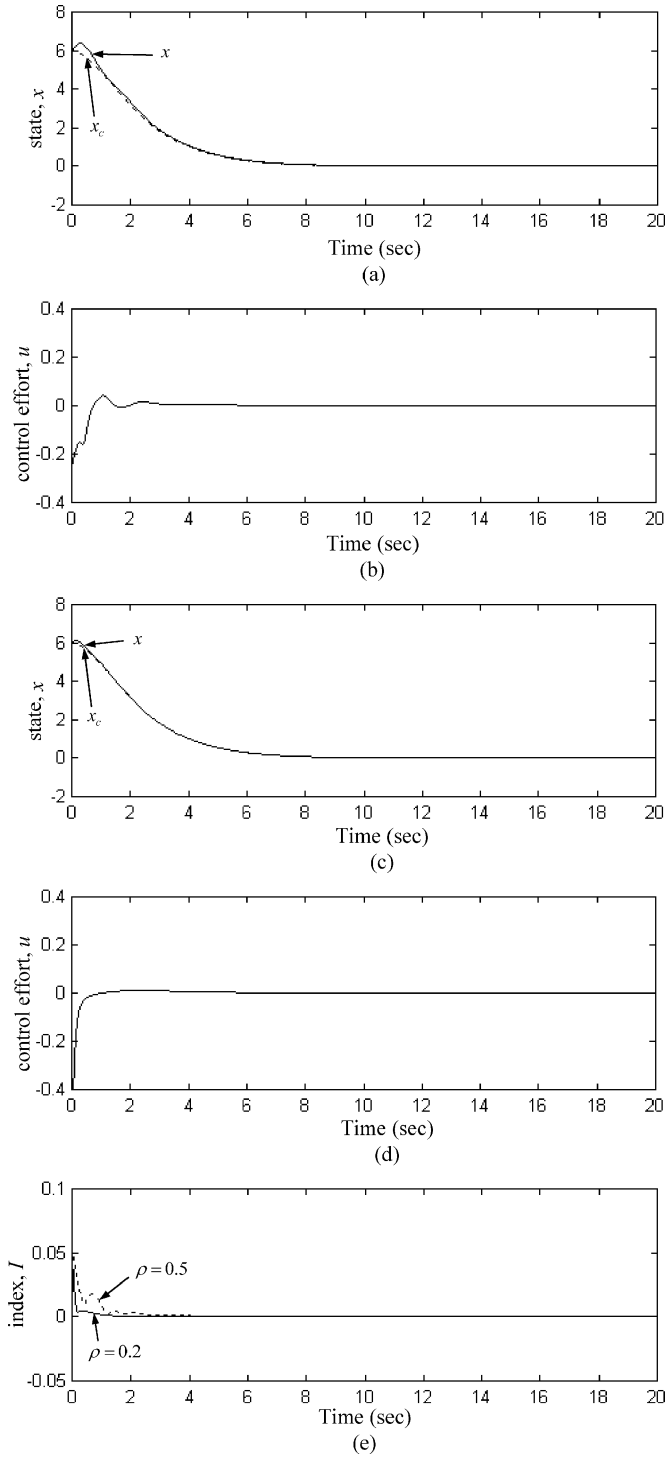

Fig. 8. Simulation results of wing-rock motion system for small initial condition.

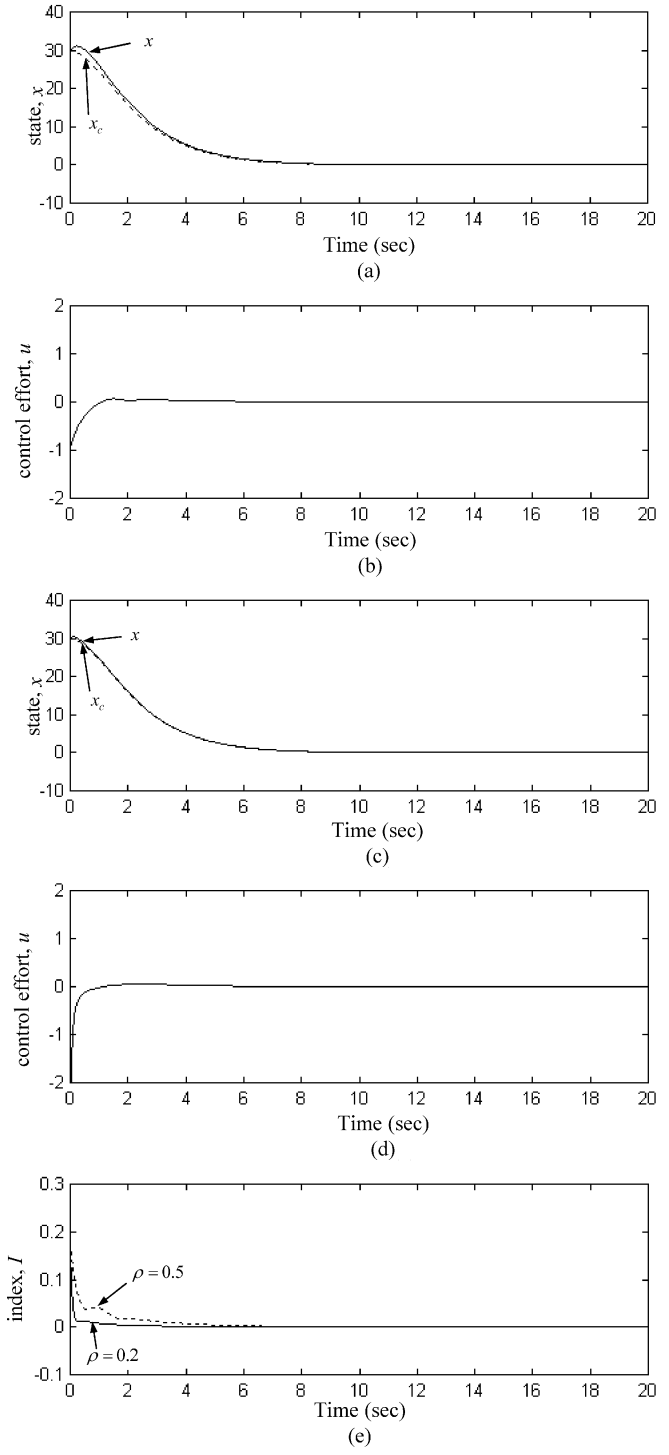

Fig. 9. Simulation results of wing-rock motion system for large initial condition.

achieve favorable identification performance, the use of adaptive backstepping control to achieve favorable control performance, and the use of L_2 robust control to achieve tracking performance with desired attenuation level. Finally, a chaotic system and a wing-rock motion system are simulated to illustrate the effectiveness of the proposed design method. Simulation results verified that the proposed WABC system can achieve favorable tracking performance of these nonlinear systems.

ACKNOWLEDGMENT

The authors would like to thank the Associate Editor and reviewers for their valuable comments.

REFERENCES

[1] M. M. Polycarpou, "Stable adaptive neural control scheme for nonlinear systems," *IEEE Trans. Autom. Control*, vol. 41, no. 3, pp. 447–451, Mar. 1996.

[2] F. J. Lin, R. J. Wai, and H. P. Chen, "A PM synchronous servo motor drive with an on-line trained fuzzy neural network controller," *IEEE Trans. Energy Conv.*, vol. 13, no. 4, pp. 319–325, Dec. 1998.
[3] H. Wang and Y. Wang, "Neural-network-based fault-tolerant control of unknown nonlinear systems," *Proc. IEE, Contr. Theory Appl.*, vol. 146, pp. 389–398, Sep. 1999.
[4] C. M. Lin and C. F. Hsu, "Neural-network-based adaptive control for induction servomotor drive system," *IEEE Trans. Ind. Electron.*, vol. 49, no. 1, pp. 115–123, Feb. 2002.
[5] ——, "Neural network hybrid control for antilock braking systems," *IEEE Trans. Neural Netw.*, vol. 14, no. 2, pp. 351–359, Mar. 2003.
[6] D. Wang and J. Huang, "Neural network-based adaptive dynamic surface control for a class of uncertain nonlinear systems in strict-feedback form," *IEEE Trans. Neural Netw.*, vol. 16, no. 1, pp. 195–202, Jan. 2005.
[7] B. Delyon, A. Juditsky, and A. Benveniste, "Accuracy analysis for wavelet approximations," *IEEE Trans. Neural Netw.*, vol. 6, no. 2, pp. 332–348, Mar. 1995.
[8] Q. Zhang, "Using wavelet network in nonparametric estimation," *IEEE Trans. Neural Netw.*, vol. 8, no. 2, pp. 227–236, Mar. 1997.
[9] D. W. C. Ho, P. A. Zhang, and J. Xu, "Fuzzy wavelet networks for function learning," *IEEE Trans. Fuzzy Syst.*, vol. 9, no. 1, pp. 200–211, Feb. 2001.
[10] S. A. Billings and H. L. Wei, "A new class of wavelet networks for nonlinear system identification," *IEEE Trans. Neural Netw.*, vol. 16, no. 4, pp. 862–874, Jul. 2005.
[11] C. K. Lin, "Adaptive tracking controller design for robotic systems using Gaussian wavelet networks," *Proc. IEE, Contr. Theory Appl.*, vol. 149, pp. 316–322, Jul. 2002.
[12] C. D. Sousa, E. M. Hemerly, and R. K. H. Galvao, "Adaptive control for mobile robot using wavelet networks," *IEEE Trans. Syst., Man, Cybern. B, Cybern.*, vol. 32, no. 4, pp. 493–504, Aug. 2002.
[13] R. J. Wai, "Development of new training algorithms for neuro-wavelet systems on the robust control of induction servo motor drive," *IEEE Trans. Ind. Electron.*, vol. 49, no. 6, pp. 1323–1341, Dec. 2002.
[14] F. J. Lin, H. J. Shieh, and P. K. Huang, "Adaptive wavelet neural network control with hysteresis estimation for piezo-positioning mechanism," *IEEE Trans. Neural Netw.*, vol. 17, no. 2, pp. 432–444, Mar. 2006.
[15] T. Zhang, S. S. Ge, and C. C. Hang, "Adaptive neural network control for strict-feedback nonlinear systems using backstepping design," *Automatica*, vol. 36, pp. 1835–1846, 2000.
[16] J. Y. Choi and J. A. Farrell, "Adaptive observer backstepping control using neural networks," *IEEE Trans. Neural Netw.*, vol. 12, no. 5, pp. 1103–1112, Sep. 2001.
[17] O. Kuljaca, N. Swamy, F. L. Lewis, and C. M. Kwan, "Design and implementation of industrial neural network controller using backstepping," *IEEE Trans. Ind. Electron.*, vol. 50, no. 1, pp. 193–201, Feb. 2003.
[18] C. M. Lin and C. F. Hsu, "Recurrent-neural-network-based adaptive backstepping control for induction servomotor," *IEEE Trans. Ind. Electron.*, vol. 52, no. 6, pp. 1677–1684, Dec. 2005.
[19] B. S. Chen and C. H. Lee, "H^∞ tracking design of uncertain nonlinear SISO systems: Adaptive fuzzy approach," *IEEE Trans. Fuzzy Syst.*, vol. 4, no. 1, pp. 32–43, Feb. 1996.
[20] W. Y. Wang, M. L. Chan, C. C. J. Hsu, and T. T. Lee, "H^∞ tracking-based sliding mode control for uncertain nonlinear systems via an adaptive fuzzy-neural approach," *IEEE Trans. Syst., Man, Cybern. B, Cybern.*, vol. 32, no. 4, pp. 483–492, Aug. 2002.
[21] C. L. Lin and T. Y. Lin, "Approach to adaptive neural net-based H^∞ control design," *Proc. IEE, Contr. Theory Appl.*, vol. 149, pp. 331–342, Jul. 2002.
[22] J. E. Slotine and W. Li, *Applied Nonlinear Control*. Englewood Cliffs, NJ: Prentice-Hall, 1991.
[23] K. Y. Lian, P. Liu, T. S. Chiang, and C. S. Chiu, "Adaptive synchronization design for chaotic systems via a scalar driving signal," *IEEE Trans. Circuits Syst. I, Fundam. Theory Appl.*, vol. 49, no. 1, pp. 17–27, Jan. 2002.
[24] C. E. Lan, Y. Chen, and K. J. Lin, "Experimental and analytical investigations of transonic limit-cycle oscillations of a flaperon," *J. Aircraft*, vol. 32, pp. 905–910, 1995.
[25] C. M. Lin and C. F. Hsu, "Recurrent neural network adaptive control of wing rock motion," *J. Guid. Control Dyn.*, vol. 25, pp. 1163–1165, 2002.

Chun-Fei Hsu (M'05) received the B.S., M.S., and Ph.D. degrees in electrical engineering from Yuan-Ze University, Taiwan, Chung Li, R.O.C., in 1997, 1999, and 2002, respectively.

After graduation, he joined the Department of Electrical and Control Engineering, National Chiao-Tung University (NCTU), Hsinchu, Taiwan, R.O.C.. During 2002–2006, he was a postdoctoral student with Professor Tsu-Tian Lee in the area of a virtual-reality dynamic simulator and an intelligent transportation system. His research interests include servomotor drives, adaptive control, flight control, and intelligent control using fuzzy system and neural network technologies.

Chih-Min Lin (S'86–M'87–SM'99) received the B.S. and M.S. degrees in control engineering and the Ph.D. degree in electronics engineering from National Chiao Tung University (NCTU), Hsinchu, Taiwan, R.O.C., in 1981, 1983, and 1986, respectively.

During 1986–1992, he was with the Chung Shan Institute of Science and Technology, Lungt'an, Taoyuan County, Taiwan, R.O.C., as a Deputy Director of System Engineering of a missile system. He also served concurrently as an Associate Professor at NCTU and Chung Yuan University, Chung Li, Taiwan, R.O.C. He joined the faculty of the Department of Electrical Engineering, Yuan-Ze University, Chung Li, Taiwan, R.O.C., in 1993, and is currently a Professor of Electrical Engineering. He also served as the Committee Member of Chinese Automatic Control Society and the Deputy Chairman of IEEE Control Systems Society, Taipei Section. During 1997–1998, he was the Honor Research Fellow in the University of Auckland, Auckland, New Zealand. His research interests include guidance and flight control, intelligent control, and systems engineering.

Tsu-Tian Lee (M'87–SM'89–F'97) was born in Taipei, Taiwan, R.O.C., in 1949. He received the B.S. degree in control engineering from the National Chiao-Tung University (NCTU), Hsinchu, Taiwan, R.O.C., in 1970, and the M.S. and Ph.D. degrees in electrical engineering from the University of Oklahoma, Norman, in 1972 and 1975, respectively.

In 1975, he was appointed Associate Professor and in 1978 Professor and Chairman of the Department of Control Engineering at NCTU. In 1981, he became a Professor and Director of the Institute of Control Engineering, NCTU. In 1986, he was a Visiting Professor and in 1987 a Full Professor of electrical engineering at the University of Kentucky, Lexington. In 1990, he was a Professor and Chairman of the Department of Electrical Engineering, National Taiwan University of Science and Technology (NTUST), Taipei, Taiwan, R.O.C. In 1998, he became the Professor and Dean of the Office of Research and Development, NTUST. Since 2000, he has been with the Department of Electrical and Control Engineering, NCTU, where he is now a Chair Professor. Since 2004, he has been with the National Taipei University of Technology (NTUT), Taipei, Taiwan, R.O.C., where he is now the President.

Prof. Lee received the Distinguished Research Award from the National Science Council, R.O.C., in 1991–1998, the Academic Achievement Award in Engineering and Applied Science from the Ministry of Education, R.O.C., in 1997, the National Endow Chair from the Ministry of Education, R.O.C., in 2003, and the TECO Science and Technology Award from TECO Technology Foundation, in 2003. He was elected to the grade of IEE Fellow in 2000, respectively. He became a Fellow of New York Academy of Sciences (NYAS) in 2002. He has served as Member of Technical Program Committee and Member of Advisory Committee for many IEEE sponsored international conferences. He is now the Vice President of Membership, a member of the Board of Governors, and the Newsletter Editor for the IEEE Systems, Man, and Cybernetics Society.